

# Micromachine-Enabled Capture and Isolation of Cancer Cells in Complex Media\*\*

Shankar Balasubramanian, Daniel Kagan, Che-Ming Jack Hu, Susana Campuzano, M. Jesus Lobo-Castañon, Nicole Lim, Dae Y. Kang, Maria Zimmerman, Liangfang Zhang,\* and Joseph Wang\*

Circulating tumor cells (CTCs) are the primary entities responsible for spawning cancer metastasis. Detection of CTCs provides an indicator for the clinical diagnosis and prognosis of various types of cancers. Several approaches, based primarily on flowing the sample through antibody-coated magnetic beads<sup>[1]</sup> or microchip<sup>[2,3]</sup> surfaces, have been described for isolating and counting CTCs. However, these approaches require extensive sample preparation and/or complex surface microstructures to detect the extremely low abundance of CTCs in blood.<sup>[3,4]</sup> In this study we describe an immuno-micromachine-based approach for in vitro isolation of cancer cells that holds promise for direct CTC detection without sample preprocessing.

Recent progress in the field of man-made nanomachines,<sup>[5]</sup> particularly major advances in the power, efficiency, motion control, and versatility of artificial nanomotors,<sup>[6]</sup> have opened the door to new and important biomedical applications ranging from drug delivery<sup>[7]</sup> to biosensing.<sup>[8]</sup> Autonomously moving synthetic nanomotors have recently been employed for the pickup and transport of diverse payloads, mostly through magnetic or electrostatic interactions.<sup>[9]</sup> Extending the scope of chemically powered nanomotors to physiological conditions is a key challenge since such nanomotors are commonly incompatible with the high ionic strength environment of biological fluids. Catalytic rolled-up microtube rockets, propelled by the recoiling force of accumulated gas bubbles,<sup>[6a,9d,e,10]</sup> are particularly attractive for isolating and transporting cancer cells for downstream analysis as they possess the necessary towing force to carry

large mammalian cells. Here we demonstrate that these microrockets overcome previous constraints to locomotion in biological fluids and are readily functionalized with an antibody specific for antigenic surface proteins expressed on cancer cells, such as anti-carcinoembryonic antigen (anti-CEA) monoclonal antibody (mAb).<sup>[11]</sup> CEA is used as a targeting antigen because it is one of the most common antigens among cancer cells, being overexpressed in approximately 95 % of colorectal, gastric, and pancreatic cancers.<sup>[12]</sup> Figure 1 conceptually illustrates the pickup and transport of

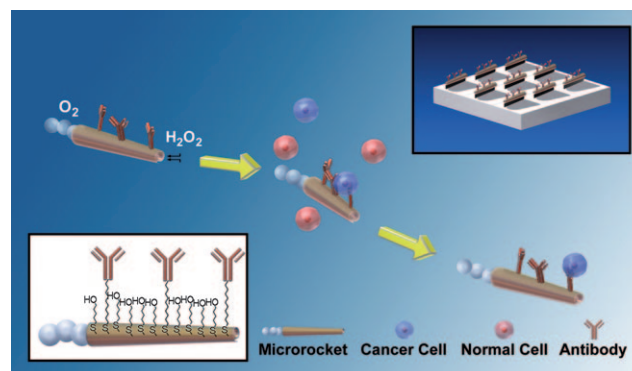


**Figure 1.** Microrockets for capture and isolation of cancer cells. Upon encountering the cells, the anti-CEA mAb-modified microrockets recognize the CEA surface antigens on the target cancer cells, allowing their selective pickup and transport. The top-right and bottom-left insets illustrate the preparation of the Ab-modified microrockets and their functionalization, respectively.

[\*] Dr. S. Balasubramanian,<sup>[†]</sup> D. Kagan,<sup>[†]</sup> C.-M. Jack Hu, Dr. S. Campuzano, Dr. M. J. Lobo-Castañon, N. Lim, D. Y. Kang, M. Zimmerman, Dr. L. Zhang, Prof. J. Wang  
Department of NanoEngineering  
University of California—San Diego, La Jolla, CA 92093 (USA)  
Fax: (+1) 858-534-9553  
E-mail: zhang@ucsd.edu  
josephwang@ucsd.edu

[†] These authors contributed equally to this work.

[\*\*] This work was supported by the National Science Foundation (award number CBET 0853375 to J.W.) and by the National Institutes of Health (grant number U54A119335 to L.Z.). M.J.L.C. thanks the University of Oviedo and the Spanish MICINN (PR 2009-0430). The authors thank M. Benchimol, B. Chuluun, and Prof. S. Esener for their help.

Supporting information for this article (including all experimental procedures) is available on the WWW under <http://dx.doi.org/10.1002/anie.201100115>.

cancer cells by microrockets. The conjugation of the anti-CEA mAb to the outer gold surface of the microrockets is accomplished through carboxy-terminated groups from a binary self-assembled monolayer (SAM) using *N*-(3-dimethylaminopropyl)-*N*-ethylcarbodiimide/*N*-hydroxysuccinimide (EDC/NHS) for amidation (see the inset in Figure 1 and the Experimental Section for details).

Practical cancer-cell-sorting applications require that effective motor propulsion is maintained in relevant physiological fluids. For example, Figure 2 and the corresponding video 1 in the Supporting Information illustrate the movement of the mAb-coated microrocket in human serum (diluted 1:4 to include the microrockets and the fuel).

These images show a long trail of microbubbles, catalytically generated on the inner platinum surface and released

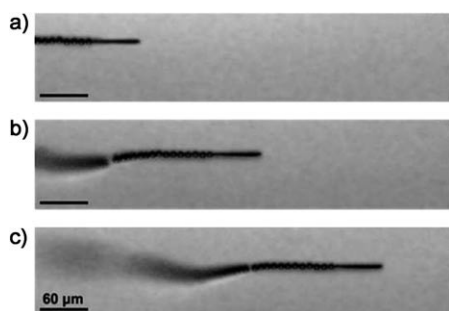


**Figure 2.** Motion in human serum. Time-lapse images, taken from video 1, showing the motion of an anti-CEA mAb-coated microrocket in human serum at 2 s intervals (a–c). Conditions: diluted human serum containing 7.5% (w/v)  $\text{H}_2\text{O}_2$  and 1% (w/v) sodium cholate.

from the rear of the microtube. Such ejection of bubbles propels the microrocket in the diluted serum medium at a relatively high speed of about  $85 \mu\text{m s}^{-1}$ . The sandwiched ferromagnetic (Fe) layer of the microrocket (see the Experimental Section) offers convenient guidance of the microrocket through tuning of the external magnetic-field direction. To facilitate effective propulsion and navigation in such biological media (even after the surface functionalization) the thickness of the Fe layer was increased at least three times compared to that in previously described microrockets.<sup>[6a,9d,10a]</sup>

These mAb-functionalized microrockets can selectively bind to target cancer cells and then effectively transport them in phosphate-buffered saline (PBS) and serum. For example, the time-lapse images of Figure 3 along with the corresponding video clips (video 2 in the Supporting Information) display the pickup of a pancreatic cancer cell bearing the antigen (CEA+) by the anti-CEA mAb-modified microrocket in PBS (a) and diluted human serum (b). These images and videos demonstrate the movement of the microrocket towards the CEA+ cell (top panel), the dynamic capture of the cell (middle panel), and subsequent directed travel of the cancer-cell-loaded micromotor over a preselected path

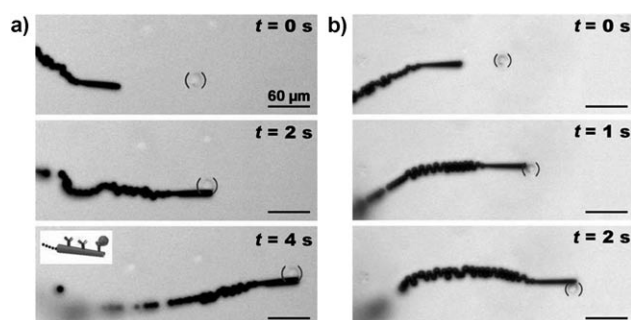


**Figure 3.** Pickup and transport in PBS and diluted serum. Time-lapse images—taken from video 2—demonstrating the pickup and transport of a CEA+ pancreatic cancer cell by an anti-CEA mAb-modified microrocket in PBS (a) and human serum (b) at intervals of 2 and 1 s, respectively. Conditions: a)  $1 \times$  PBS buffer (pH 7.4) and b) diluted human serum, containing 7.5% (weight/volume)  $\text{H}_2\text{O}_2$  and 1% (w/v) sodium cholate. The CEA+ cells are accented by using solid parentheses.

(bottom panel) without compromising the trajectory of the microrocket movement. The high speed of the microrocket is only slightly affected by the cell loading (e.g., decreasing from  $85$  to  $80 \mu\text{m s}^{-1}$  in serum environment), reflecting its high towing force. Such successful pickup is observed at nearly 80% ( $n=43$ ) of the time during the first interaction between the modified microrockets and the CEA+ cells while the efficiency decreases to 70% in serum. The cells were not observed to nonspecifically bind to the microrocket during the various control experiments except in the case when they were sucked up into the opening of the microrocket (representing 2% of the time,  $n=120$ ).

The substantial force essential for transporting a relatively large ( $\approx 16 \mu\text{m}$ ) cancer cell reflects the bubble recoiling propulsion mechanism of the microrockets. The velocity-dependent drag force of the microrockets has been estimated from Stokes' law (see the Supporting Information for detailed analysis). The minimum force necessary for transporting such large cells at one body length per second is 2.5 pN (see Table S1 in the Supporting Information), which is an order of magnitude larger than the force generated by previously developed magnetically or chemically powered nano/micro-scale motors.<sup>[7,13]</sup>

Unmodified microrockets usually move at a high speed of up to  $2 \text{ mm s}^{-1}$  in PBS media (not shown), thus exerting a force up to 250 pN. However, after the surface modification with the antibody these microrockets travel in the same bulk media at a speed of up to  $150 \mu\text{m s}^{-1}$ , thus generating an estimated force of about 18 pN. Partial blocking by adsorbed proteins and sulfur poisoning of the catalytic platinum surface<sup>[14]</sup> may account for this diminished speed. In the presence of diluted serum, the maximum microrocket speed in the bulk solution further drops to about  $100 \mu\text{m s}^{-1}$ , reflecting the increased solution viscosity. Even at the lower speed, the microrockets have sufficient force ( $> 13 \text{ pN}$ ) to overcome the additional drag force caused by the capture of a cancer cell and we observed that they can transport the cell over long periods ( $> 60 \text{ s}$ ; see video 3 in the Supporting Information for a shorter time period and distance). The lower microrocket speed is advantageous for the cell capture and transport as it reduces the shear stress and allows for sufficient antigen/antibody interaction. The upper limit of the microrocket speeds in PBS and serum results in estimated shear stresses of 2.3 and  $1.7 \text{ dyn cm}^{-2}$ , respectively (see Table S2 in the Supporting Information). Such values have been commonly observed when flowing cells are selectively captured in microfluidic devices through antibody interactions.<sup>[2,15]</sup>

The specific binding of the CEA+ cancer cells to anti-CEA mAb-modified microrockets was verified by control experiments. We studied the interactions between anti-CEA mAb-modified microrockets and the pancreatic cancer cells without antigen (CEA−) and between SAM-modified microrockets without the mAb and the CEA+ pancreatic cancer cells (see Figure 4 and video 4 in the Supporting Information; see the Experimental Section for preparation of these “control” microrockets). The results illustrate that none of the control microrockets has the capability of picking up cancer cells (Figure 4c–h). Only the anti-CEA mAb-modified

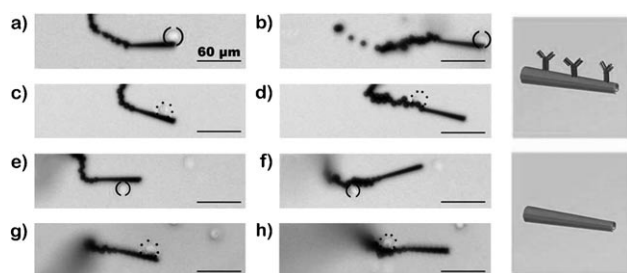


**Figure 4.** Selectivity. Time-lapse images—taken from video 4—during (left) and after (right) the interaction between anti-CEA mAb-modified (a–d) and unmodified (e–h) microrockets with CEA+ cancer cells (a, b, e and f; solid parentheses) and CEA– cancer cells (c, d, g and h; dotted parentheses). The conditions are the same as given in the caption of Figure 3 a.

microrockets are able to capture the target CEA+ cancer cells (Figure 4a,b). For these control experiments, we deliberately selected microrockets that moved slower along the glass slide interface (average speed of  $45 \mu\text{m s}^{-1}$ ) as a way to minimize the exerting shear stress ( $0.7 \text{ dyne cm}^{-2}$ , see Table S2 in the Supporting Information) and maximize the microrocket/cell interaction time. We further confirmed that the interaction between the CEA+ cell and the mAb-modified microrocket was strong and specific by oscillating the pair vigorously using a magnet (see video 5 in the Supporting Information). These results, along with the subsequent studies involving cells mixture (CEA+ and CEA– cells) clearly demonstrate that the capture of the cancer cell occurs through the specific antigen recognition.

The viability of the cells under the conditions used in the present study was examined using the trypan blue exclusion assay (see Table S3 and Figure S2 in the Supporting Information). The cancer cells were subject to PBS solutions containing various levels of the peroxide fuel. While more than half of the cells remained viable for over 10 minutes at a peroxide level of 8%, the majority of the cells (>90%) remained viable after 1 hour of immersion in a 2% peroxide solution. Such time windows would allow for the retrieval of cells for subsequent analysis. We also observed the ability of the mAb-coated microrockets to bind to dead CEA+ cells or their cellular membrane fragments. Therefore, from the perspective of cell detection, these microrockets can identify any CEA-expressing cell regardless of its viability.

The ability of the anti-CEA mAb-modified microrockets to identify and isolate target cancer cells was further demonstrated using a mixture of green fluorescently stained CEA+ cancer cells and unstained CEA– cancer cells. As shown in the overlay images of Figure 5 (taken from video 6 in the Supporting Information), the microrocket first closely interacts with the CEA– cell (steps 1 and 2), hitting and displacing it to a different focal plane (owing to a lack of reaction). After such direct contact without pickup of the CEA– cell, the microrocket captures and transports a CEA+ cell (steps 4 and 5). The CEA+ cell is tightly bound to the modified microrocket during deliberate oscillations. This selective binding was confirmed by exposing the sample to a blue light (460 nm), which excites the CEA+ cells stained

with a green fluorescent dye (step 5). The CEA– cells are indicated by a lack of fluorescence while exposed to blue light at the beginning of the video. A microrocket moving along the bottom plane was chosen; because of its reduced speed we can properly guide the microrocket and distinguish the fluorescent CEA+ cells (from the CEA– cells on the same plane) under the  $40\times$  magnification. A similar experiment involving the incubation of modified microrockets (without fuel) with a mixture of CEA+ and CEA– cells further demonstrates the selectivity of the mAb-modified microrocket (Figure S3 in the Supporting Information). These experiments confirm the ability of microrockets to selectively recognize target cancer cells in cell mixtures.

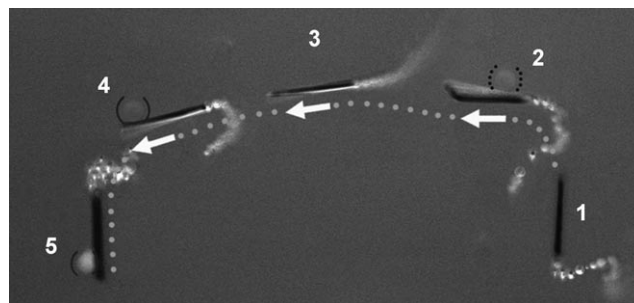


**Figure 5.** Isolation of a CEA+ cell in a mixture of cells. The overlay images—taken from video 6 in the Supporting Information—show sequential steps (1–5) of movement of the anti-CEA mAb-modified microrocket in a mixture of CEA+ and CEA– cells (solid and dotted parentheses, respectively). For clear visualization, step 5 has been slightly displaced. The conditions are the same as given in the captions of Figures 3 a and 4.

In conclusion, we have demonstrated a new *in vitro* strategy for isolating cancer cells based on the selective binding and transport ability of mAb-functionalized micro-engine rockets. These microrockets can be readily functionalized with targeting ligands such as mAb for highly specific cancer cell selection and provide sufficient propulsive force for the efficient transport of the captured target cells in complex media. While the concept has been illustrated for the capture of pancreatic cancer cells, it could be expanded to other cancer cell lines. Such microrocket-based selective capture and transport of tumor cells without preprocessing biological samples holds great promise for extracting CTCs from biological fluids and hence for the early diagnosis of cancer and its recurrence. The autonomous transport properties of the microrockets in viscous fluids such as serum might eliminate the multiple preparatory steps required for the existing magnetic bead-based systems.<sup>[2]</sup> In addition, we could increase the efficiency of the viable cell separation process by altering the interactions (i.e., by controlling the shear stress). This micromachine-based cell manipulator and sorter could be readily incorporated in microchannel networks for creating integrated microchip devices. Such microchips will rely on the active transport of multiple immuno-micromachines in a blood sample reservoir to induce numerous interactions, high capture efficiency, and single-step isolation of CTCs. Fur-

thermore, this can be extended to accumulating CTCs in a predefined “collection” area by detaching the captured cells.

Received: January 7, 2011  
Published online: April 7, 2011

**Keywords:** antibodies · cancer · micromachines

- [1] E. I. Galanzha, E. V. Shashkov, T. Kelly, J.-W. Kim, L. Yang, V. P. Zharov, *Nat. Nanotechnol.* **2009**, *4*, 855–860.
- [2] S. Nagrath, L. V. Sequist, S. Maheswaran, D. W. Bell, D. Irimia, L. Ulkus, M. R. Smith, E. L. Kwak, S. Digumarthy, A. Muzikansky, P. Ryan, U. J. Balis, R. G. Tompkins, D. A. Haber, M. Toner, *Nature* **2007**, *450*, 1235–1239.
- [3] A. A. Adams, P. I. Okagbare, J. Feng, M. L. Hupert, D. Patterson, J. Göttert, R. L. McCarley, D. Nikitopoulos, M. C. Murphy, S. A. Soper, *J. Am. Chem. Soc.* **2008**, *130*, 8633–8641.
- [4] A. L. Allan, M. Keeney, *J. Oncol.* **2010**, 426218.
- [5] a) T. Mirkovic, N. S. Zacharia, G. D. Scholes, G. A. Ozin, *ACS Nano* **2010**, *4*, 1782–1789; b) J. Wang, *ACS Nano* **2009**, *3*, 4–9; c) T. E. Mallouk, A. Sen, *Sci. Amer.* **2009**, *300*, 72–77.
- [6] a) A. A. Solovev, Y. F. Mei, E. Bermúdez Ureña, G. S. Huang, O. G. Schmidt, *Small* **2009**, *5*, 1688–1692; b) J. Wang, K. M. Manesh, *Small* **2010**, *6*, 338–345; c) W. F. Paxton, S. Sundararajan, T. E. Mallouk, A. Sen, *Angew. Chem.* **2006**, *118*, 5546–5556; *Angew. Chem. Int. Ed.* **2006**, *45*, 5420–5429; d) S. J. Ebbens, J. R. Howse, *Soft Matter* **2010**, *6*, 726–738.
- [7] D. Kagan, R. Laocharoensuk, M. Zimmerman, C. Clawson, S. Balasubramanian, D. Kang, D. Bishop, S. Sattayasamitsathit, L. Zhang, J. Wang, *Small* **2010**, *6*, 2741–2747.
- [8] J. Wu, S. Balasubramanian, D. Kagan, K. M. Manesh, S. Campuzano, J. Wang, *Nat. Commun.* **2010**, DOI: 10.1038/ncomms1035.
- [9] a) S. Sundararajan, P. E. Lammert, A. W. Zudans, V. H. Crespi, A. Sen, *Nano Lett.* **2008**, *8*, 1271–1276; b) J. Burdick, R. Laocharoensuk, P. M. Wheat, J. D. Posner, J. Wang, *J. Am. Chem. Soc.* **2008**, *130*, 8164–8165; c) S. Sundararajan, S. Sengupta, M. E. Ibele, A. Sen, *Small* **2010**, *6*, 1479–1482; d) A. A. Solovev, S. Sanchez, M. Pumera, Y. F. Mei, O. G. Schmidt, *Adv. Funct. Mater.* **2010**, *20*, 2430–2435; e) S. Sánchez, A. A. Solovev, S. Schulze, O. G. Schmidt, *Chem. Commun.* **2011**, 47, 698–700.
- [10] a) Y. Mei, G. Huang, A. A. Solovev, E. Bermúdez Ureña, I. Mönch, F. Ding, T. Reindl, R. K. Y. Fu, P. K. Chu, O. G. Schmidt, *Adv. Mater.* **2008**, *20*, 4085–4090; b) K. M. Manesh, M. Cardona, R. Yuan, M. Clark, D. Kagan, S. Balasubramanian, J. Wang, *ACS Nano* **2010**, *4*, 1799–1804.
- [11] Z.-R. Shi, D. Tacha, S. H. Itzkowitz, *J. Histochem. Cytochem.* **1994**, *42*, 1215–1219.
- [12] V. Zieglschmid, C. Hollmann, O. Böcher, *Crit. Rev. Clin. Lab. Sci.* **2005**, *42*, 155–196.
- [13] L. Zhang, J. J. Abbott, L. Dong, K. E. Peyer, B. E. Kratochvil, H. Zhang, C. Bergeles, B. J. Nelson, *Nano Lett.* **2009**, *9*, 3663–3667.
- [14] C. H. Bartholomew, P. K. Agrawal, J. R. Katzer in *Advances in Catalysis*, Vol. 31, Academic Press, **1982**, pp. 135–242.
- [15] B. D. Plouffe, T. Kniazeva, J. E. Mayer, Jr., S. K. Murthy, V. L. Sales, *FASEB J.* **2009**, *23*, 3309–3314.